Eur. Phys. J. B **2**, 131–142 (1998)

THE EUROPEAN PHYSICAL JOURNAL B

Energy-transfer and quantum trajectories in quasi-molecular networks

C.M. Granzow[a], A. Liebman, and G. Mahler

Institut für Theoretische Physik, Universität Stuttgart, Pfaffenwaldring 57, 70550 Stuttgart, Germany

Received: 21 July 1997 / Received in final form: 10 November 1997 / Accepted: 27 October 1997

Abstract. Continuous measurement models are conveniently based on master equations specified by the respective Hamiltonian and appropriate environment operators. As demonstrated by stochastic unraveling, the latter specify the dynamical process rather than static detection modes. We show that certain environment operators acting on a simple system may, in fact, require extended networks for implementation: Their Hamilton parameters re-appear in the effective environment operators of the reduced model. The resulting quantum trajectories typically involve competing paths, which may give rise to different fluctuation and noise properties even when the corresponding ensemble behavior is practically the same.

PACS. 42.50.Lc Quantum fluctuations, quantum noise, and quantum jumps – 06.20.Dk Measurement and error theory

1 Introduction

A quantum system is routinely defined by its Hamiltonian, which, at the same time, controls its unitary dynamical evolution. This Hamiltonian, however, does not suffice to specify the dynamics of an open quantum system. In the Markovian master equation [1] the influence of the environment is taken into account by means of so-called environment-operators, which act local in time. They are not unique, though: Under certain transformations of these operators the master equation is invariant [2], if parameters are transformed correspondingly.
In general, however, this invariance does not carry over to stochastic unravelings [3]: Qualitatively *different* quantum trajectories may thus correspond to the *same* ensemble solution. This ambiguity is of no concern, as long as those unravelings are employed merely as technical means to solve the ensemble master equation, *i.e.* to find the time-dependent density matrix by averaging over the trajectories. The situation changes, though, if one is interested also in noise-properties and/or the interpretation of individual measurement traces. Then the trajectories should reflect the way the system is actually measured. However, these different processes specified by environment operators must be selected somehow on a physical basis. One may wonder, how any realistic model could be specific enough to allow for such a diversity.

We will show that the quantum system itself may come for rescue: Under appropriate conditions certain Hamilton–model parameters of a *full* network appear as respective transformation parameters for the environment operators in a *reduced* description. Such reduced models result after subsystems have been eliminated adiabatically. They readily go beyond simple rate equation approaches.

Insofar as these measurement models require extended networks for implementation, the conventional scenario of a quantum system being embedded in a classical environment (including means for observation) needs refinements: The system extensions are quantum but, in a sense, belong to the environment in that they help to define effective environment operators.

2 Basic notation

Defining on an orthonormalized complete set of states $|i\rangle$, $i = 1, 2, \ldots, n$ (n finite) the n^2 basic operators

$$\hat{\mathrm{P}}_{ij} = |i\rangle\langle j| \,, \tag{1}$$

we can write the density operator of the system under consideration as

$$\hat{\rho} = \sum_{i,j} \rho_{ij} \hat{\mathrm{P}}_{ij} \,, \tag{2}$$

where $\rho_{ij} = \mathrm{Tr}\{\hat{\rho}\hat{\mathrm{P}}_{ji}\} = \langle i|\,\hat{\rho}\,|j\rangle$ is the density matrix.
The influence of the environment will be described by the environment-operators, $\hat{\mathrm{G}}_l$; they can be taken to be traceless

$$\mathrm{Tr}\{\hat{\mathrm{G}}_l\} = 0 \tag{3}$$

[a] e-mail: claus@theo.physik.uni-stuttgart.de

and orthogonalized [4]

$$\mathrm{Tr}\{\hat{\mathrm{G}}_l \hat{\mathrm{G}}_m^+\} = \delta_{lm}\,. \tag{4}$$

Here, $l, m = 1, 2, \ \ldots, n^2-1$. A possible choice for the $\hat{\mathrm{G}}_l$ are the Hermitian SU(n) - generators (normalized to factor 2 rather than unity). Closer to concrete damping models, though, are the non-Hermitian transition-operators $\hat{\mathrm{P}}_{ij}$, $i \neq j$; these will underly the following examples. Based on these environment-operators the Lindblad master equation reads [5,6]

$$\frac{\partial}{\partial t}\hat{\rho}(t) = -\frac{\mathrm{i}}{\hbar}[\hat{\mathrm{H}}, \hat{\rho}] + \hat{\mathcal{L}}^{(1)}_{\mathrm{incoh}}\hat{\rho} + \hat{\mathcal{L}}^{(2)}_{\mathrm{incoh}}\hat{\rho}\,, \tag{5}$$

with the Lindblad-operators given by

$$\hat{\mathcal{L}}^{(1)}_{\mathrm{incoh}}\hat{\rho} = \sum_{l,\ l'=1}^{n^2-1} D_{ll'}\hat{\mathrm{G}}_l\hat{\rho}\hat{\mathrm{G}}_{l'}^+\,, \tag{6}$$

$$\hat{\mathcal{L}}^{(2)}_{\mathrm{incoh}}\hat{\rho} = -\frac{1}{2}\sum_{l,\ l'=1}^{n^2-1} D_{ll'}\left[\hat{\mathrm{G}}_{l'}^+\hat{\mathrm{G}}_l\hat{\rho} + \hat{\rho}\hat{\mathrm{G}}_{l'}^+\hat{\mathrm{G}}_l\right]. \tag{7}$$

The parameter matrix $D_{ll'}$ is Hermitian and positive semidefinite, $D_{ll'} = (D_{l'l})^*$ (*cf.* Ref. [4]).

3 Invariance properties of the Lindblad-master equation

3.1 Diagonalization of the parameter matrix D

The operators $\hat{\mathrm{G}}_l$ form a complete basis to represent any traceless operator $\hat{\mathrm{B}}$:

$$\hat{\mathrm{B}} = \sum_m \hat{\mathrm{G}}_m \mathrm{Tr}\{\hat{\mathrm{B}}\hat{\mathrm{G}}_m^+\}. \tag{8}$$

In particular, a new orthonormalized basis $\hat{\tilde{\mathrm{G}}}$ can be represented by

$$\hat{\tilde{\mathrm{G}}}_l = \sum_m \hat{\mathrm{G}}_m U_{lm} \tag{9}$$

where $U_{lm} = \mathrm{Tr}\{\hat{\tilde{\mathrm{G}}}_l\hat{\mathrm{G}}_m^+\}$ has to be unitary. The representation of the master equation in $\hat{\mathrm{G}}_m$ together with the following unitary transformation of the parameter matrix

$$D_{ll'} = \sum_{m,m'} U_{lm}\tilde{D}_{mm'}U^*_{lm'}\,, \tag{10}$$

will cause that the Lindblad-operators retain their original form.

These operators can thus be expressed by any orthogonal complete set of environment-operators: For any such representation the ensemble solution of the master equation will be the same [7].

Of special interest is the representation in which $\tilde{D}_{mm'}$ becomes diagonal, which always exists as $D_{ll'}$ is a Hermitian matrix. The transformed parameter matrix $\tilde{D}_{mm'}$ then reads

$$\tilde{D}_{mm'} = W_m\delta_{mm'}\,, \tag{11}$$

with the diagonal terms W_m as the eigenvalues of $D_{ll'}$. These are always non-negative and can be interpreted as transition rates for a set of up to (n^2-1) independent stochastic processes. The corresponding environment-operators will be denoted by $\hat{\mathrm{F}}_m = \hat{\tilde{\mathrm{G}}}_m$; only those are relevant for which $W_m \neq 0$.

3.2 Effective environment-operators

Given now in the diagonal representation a set of operators $\hat{\mathrm{F}}_l$ with more than one eigenvalue $W_l \neq 0$, the choice of environment-operators is not unique, though, if we relax the orthogonality condition. To see this, let us combine the transition rate W_l with the environment-operator (Ref. [2])

$$\hat{\mathrm{L}}_l = \sqrt{W_l}\hat{\mathrm{F}}_l\,. \tag{12}$$

The parameter matrix then simply reduces to the unit matrix and the master equation reads in this case:

$$\frac{\partial}{\partial t}\hat{\rho}(t) = -\frac{i}{\hbar}[\hat{\mathrm{H}}, \hat{\rho}] + \sum_i(\hat{\mathrm{L}}_i\hat{\rho}\hat{\mathrm{L}}_i^+ - \frac{1}{2}\hat{\mathrm{L}}_i^+\hat{\mathrm{L}}_i\hat{\rho} - \frac{1}{2}\hat{\rho}\hat{\mathrm{L}}_i^+\hat{\mathrm{L}}_i)\,. \tag{13}$$

In general, equation (4) does no longer hold. Any subsequent unitary transformation $\hat{\tilde{\mathrm{L}}}_{\mathrm{s}}(\mu) = \sum_l \hat{\mathrm{L}}_l U_{l\mathrm{s}}$ in the subspace of l with $W_l \neq 0$ will necessarily leave the parameter matrix invariant and may lead to an "oblique-angle reference frame". There are thus (infinitely many) operator sets depending on continuous parameters and accessible to stochastic unraveling while producing the same ensemble result!

Finally, we may also drop the condition (3): Starting from the diagonal representation, equation (12), we consider the change of trace according to [8]

$$\hat{\tilde{\mathrm{L}}}_l = \sqrt{W_l}(\hat{\mathrm{F}}_l + \alpha_l\hat{\mathbf{1}}), \qquad \alpha_l \quad \text{complex}\,. \tag{14}$$

In this case, for the master equation to remain unchanged for any given α_l, it is necessary to transform also the Hamilton-operator according to

$$\hat{\tilde{\mathrm{H}}} = \hat{\mathrm{H}} + \Delta\hat{\mathrm{H}}(\alpha_l)\,, \tag{15}$$

$$\Delta\hat{\mathrm{H}}(\alpha_l) = -\frac{i\hbar}{2}\sum_l \sqrt{W_l}(\alpha_l^*\hat{\mathrm{L}}_l - \alpha_l\hat{\mathrm{L}}_l^+)\,. \tag{16}$$

$\Delta\hat{\mathrm{H}}$ acts as an effective driving term, where α_l plays the role of an external field amplitude.

3.3 Quantum jump model

For the evolution of a single quantum system we follow the Monte-Carlo wavefunction approach for the simulation of a continuous measurement developed by Dalibard and Mølmer, Carmichael *et al.* [9–11].

For stochastic unraveling we require the parameter matrix $D_{ll'}$ to be diagonal and consider the set of environment-operators (*cf.* Eq. (14))

$$\begin{aligned}\hat{\tilde{\mathrm{L}}}_s &= \sum_l U_{ls}(\hat{\mathrm{L}}_l + \sqrt{W_l}\alpha_l \hat{\mathbf{1}}) \\ &= \sum_l U_{ls}\hat{\mathrm{L}}_l \;+\; \hat{\mathbf{1}}\sum_l U_{ls}\sqrt{W_l}\alpha_l \\ &= \sum_l U_{ls}\hat{\mathrm{L}}_l \;+\; \sqrt{W_s}\alpha_s\hat{\mathbf{1}}\,.\end{aligned} \tag{17}$$

Here, the last sum of equation (17) has been compressed into $\sqrt{W_s}\alpha_s$, with a formal damping rate W_s. In these $\hat{\tilde{\mathrm{L}}}_s$ the master equation is diagonal and invariant for any unitary U_{ls} and complex α_s. Each term specified by s is now interpreted to give rise to an independent stochastic process. The probability for the occurrence of an event s, $\hat\rho \to \hat\rho' = \hat{\tilde{\mathrm{L}}}_s\hat\rho\hat{\tilde{\mathrm{L}}}_s^+$ in the time interval δt ($\delta t \ll W^{-1}$) is given by

$$P_s = \mathrm{Tr}\{\hat{\tilde{\mathrm{L}}}_s\hat\rho\hat{\tilde{\mathrm{L}}}_s^+\}\delta t\,. \tag{18}$$

Between these measurement projections, which are defined by the operators $\hat{\tilde{\mathrm{L}}}_s$ (and thus are a function of the transformation), the evolution obeys the truncated master equation [12]

$$\frac{\partial}{\partial t}\hat\rho(t) = -\frac{i}{\hbar}[\hat{\tilde{\mathrm{H}}},\hat\rho] + \hat{\mathcal{L}}^{(2)}_{\mathrm{incoh}}\hat\rho = -\frac{i}{\hbar}[\hat{\mathrm{H}}_{\mathrm{eff}}\hat\rho - \hat\rho\hat{\mathrm{H}}^+_{\mathrm{eff}}]\,, \tag{19}$$

where the effective Hamiltonian is given by

$$\begin{aligned}\hat{\mathrm{H}}_{\mathrm{eff}} = \hat{\mathrm{H}} - \frac{i\hbar}{2}\sum_s [&\hat{\tilde{\mathrm{L}}}_s^+\hat{\tilde{\mathrm{L}}}_s \\ &+\sqrt{W_s}\alpha_s^*\hat{\tilde{\mathrm{L}}}_s - \sqrt{W_s}\alpha_s\hat{\tilde{\mathrm{L}}}_s^+]\,.\end{aligned} \tag{20}$$

This dynamics is, as can easily be seen, not trace preserving. So it is necessary to renormalize the state after each time step. (More efficient techniques are available, see [13].)

The problem we want to address is the implementation of these environment operators, *i.e.* of the continuous parameters U_{ls} and α_s. For this purpose we introduce "extended" systems, of which the original system (S) will appear as the part to be eventually measured, while the "rest" helps to specify the environment operators.

4 Composite systems

4.1 Network model

For composite systems (N subspaces of local dimension n_μ, $\mu = 1, 2, \ldots, N$) we conveniently use product states $|l\rangle = |i(1)\rangle \otimes |j(2)\rangle \otimes \ldots |k(N)\rangle$ and products of local projection operators $\hat{\mathrm{P}}_{ij}(\mu) = |i(\mu)\rangle\langle j(\mu)|$, respectively. We consider composite systems described by [14]

$$\hat{\mathrm{H}} = \sum_\mu \hat{\mathrm{H}}(\mu) + \sum_{\mu<\nu}\hat{\mathrm{V}}(\mu,\nu) \tag{21}$$

with $\hat{\mathrm{H}}(\mu) = \sum_i E_i^\mu \hat{\mathrm{P}}_{ii}(\mu) + \hat{\mathrm{V}}(\mu)$. Here E_i^μ is the subsystem spectrum, and $\hat{\mathrm{V}}(\mu)$ includes coupling to external (classical) fields. Applicability of the rotating wave approximation is assumed (see, *e.g.* [15]). $\hat{\mathrm{V}}(\mu,\nu)$ accounts for inter-subsystem coupling. The type of energy transfer interactions considered in this paper are summarized in Figure 1 (double lines), together with the local damping channels (dotted lines).

The set of traceless orthonormalized local operators $\hat{\mathrm{G}}_i(\mu)$, $i = 1, 2 \ \ldots n_\mu^2 - 1$, $\mu = 1, 2 \ \ldots N$, now forms a complete basis to represent any traceless single-particle-operator $\hat{\mathrm{B}}$:

$$\hat{\mathrm{B}} = \sum_{\mu=1}^{N}\sum_{m=1}^{n_\mu^2-1}\hat{\mathrm{G}}_m(\mu)\mathrm{Tr}\{\hat{\mathrm{B}}\hat{\mathrm{G}}_m^+(\mu)\}\,, \tag{22}$$

$\hat{\mathrm{B}}$ is single-particle in the sense that each term in the sum acts on but one single subsystem. (Two-particle operators would involve pairs of such local operators.) This representation applies, in particular, to sets of transformed environment operators $\hat{\tilde{\mathrm{G}}}_l$,

$$\hat{\tilde{\mathrm{G}}}_l = \sum_{\mu=1}^{N}\sum_m \hat{\mathrm{G}}_m(\mu)U^\mu_{lm}\,. \tag{23}$$

4.2 System reductions

For special parameter windows it is possible to reduce the number of subsystems without changing the relevant state space. But even then, the reduced model typically contains some additional parameters allowing for some added flexibility in the specification of what is actually being measured. Here we discuss three basic types of such an adiabatic elimination procedure.

i) In the first one we start from a $N = 2$ network coupled by [16]

$$\hat{\mathrm{V}}(1,\mathrm{S}) = \hbar C_{\mathrm{F}}\hat{\mathrm{P}}_{21}(1)\otimes\hat{\mathrm{P}}_{12}(\mathrm{S}) + \hbar {C_{\mathrm{F}}}^*\hat{\mathrm{P}}_{12}(1)\otimes\hat{\mathrm{P}}_{21}(\mathrm{S})\,. \tag{24}$$

$\hat{\mathrm{V}}(1,\mathrm{S})$ describes resonant energy transfer between subsystem (S) and (1). In system (1) there is a dissipation channel with $\hat{\mathrm{F}}(1) = \hat{\mathrm{P}}_{12}(1)$ and transition rate W^1. For $W^1 \gg |C_{\mathrm{F}}|$ system (1) is overdamped and its dynamics can be neglected. This means that the reduced system has approximately the same relevant state space as the original full network. The effective damping rate for transition $\hat{\mathrm{F}}(\mathrm{S}) = \hat{\mathrm{P}}_{12}(\mathrm{S})$ in system (S) then is (*cf.* Appendix A)

$$W^s_{\mathrm{eff}} = \frac{|C_{\mathrm{F}}|^2\, W^1}{(W^1/2)^2 + (\delta)^2}\,, \tag{25}$$

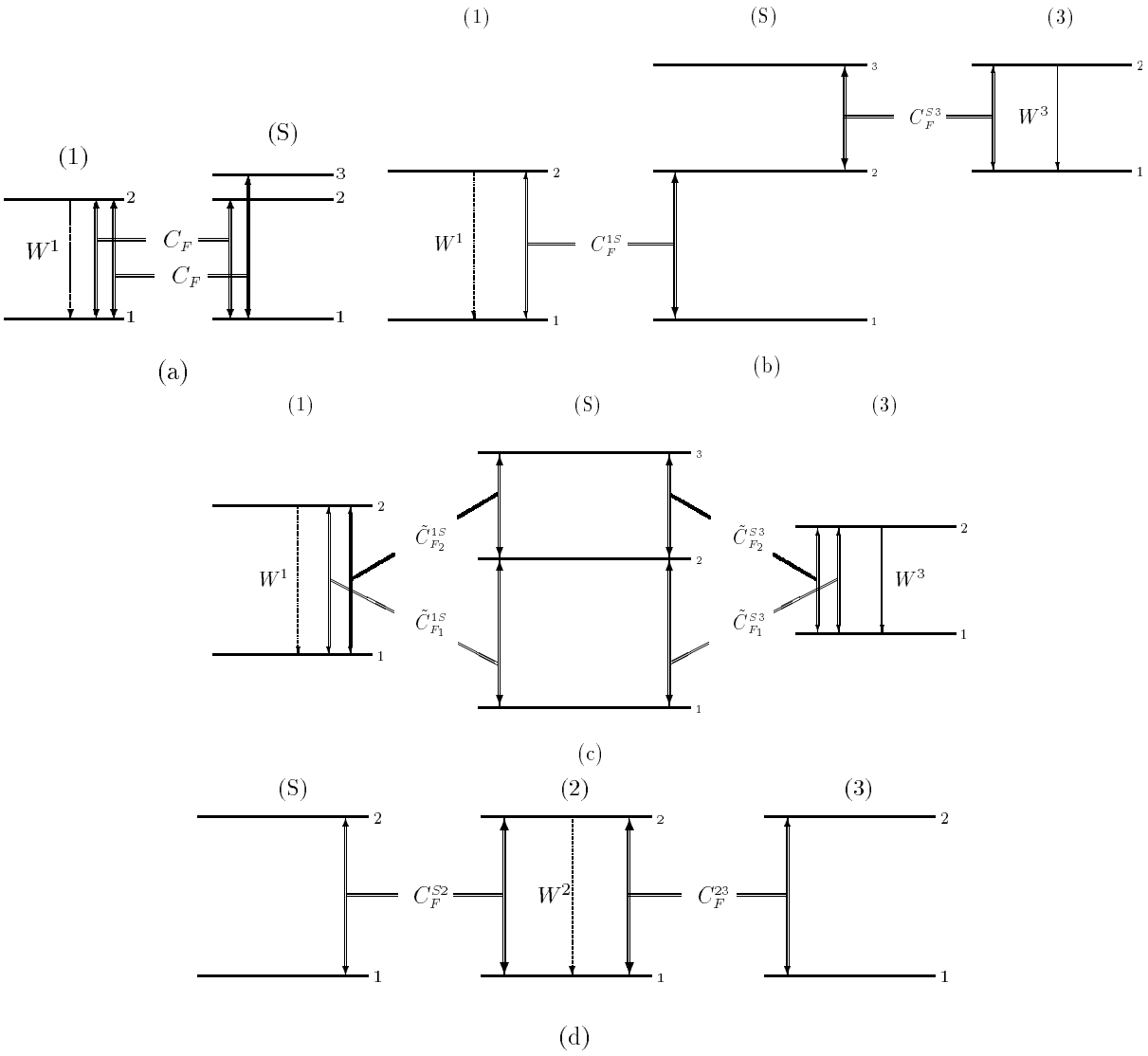

Fig. 1. N-subsystem networks. (a) $N = 2$, 2 transfer paths (double lines), 1 damping channel (dotted line). (b) $N = 3$, 2 transfer paths, 2 damping channels. (c) $N = 3$, 4 transfer paths, 2 damping channels. (d) $N = 3$, 2 transfer paths, 1 damping channel. The subsystem (S) is the one to which the network can be reduced under appropriate conditions.

where δ is the detuning between the two two-level systems. The auxiliary system (1) might be seen, *e.g.* as the two lowest levels of a photon number state of a mode, into which the spontaneous emission will occur, or, alternatively, as another molecular subsystem: in any case, this subsystem (1) could be coupled to more than one pair of levels of (S) thus giving rise to environment-operators like $\hat{\mathrm{F}}(\mathrm{S}) = c_1\hat{\mathrm{P}}_{ij}(\mathrm{S}) + c_2\hat{\mathrm{P}}_{kl}(\mathrm{S})$, where the c_i relate to the respective coupling strengths (*cf.* Fig. 1a).

ii) We now consider a $N = 3$ network, specified by (see Fig. 1d)

$$\hat{\mathrm{H}} = \hat{\mathrm{H}}(\mathrm{S}) + \hat{\mathrm{H}}(2) + \hat{\mathrm{H}}(3) + \hat{\mathrm{V}}(\mathrm{S},2) + \hat{\mathrm{V}}(3,2)\,, \qquad (26)$$

with

$$\hat{\mathrm{V}}(\mathrm{S},2) = c_1\hat{\mathrm{P}}(\mathrm{S})\hat{\mathrm{Q}}(2) + c.c.\,, \qquad (27)$$

$$\hat{\mathrm{V}}(3,2) = c_2\hat{\mathrm{P}}(3)\hat{\mathrm{Q}}(2) + c.c.\,, \qquad (28)$$

where $\hat{\mathrm{P}}(\mathrm{S})$ ($\hat{\mathrm{P}}(3)$) describes respective subsystem operators in the system (third subsystem) and $\hat{\mathrm{Q}}(2)$ acts on damped system (2). $\hat{\mathrm{V}}(\mathrm{S},2)$ and $\hat{\mathrm{V}}(3,2)$ relate to the same $\hat{\mathrm{Q}}(2)$, which thus can be taken in front of the combination: Eliminating the overdamped system (2) leads to a generalized measurement model for an effective $N = 2$ network with

$$\hat{\mathrm{F}}(\mathrm{S},3) = c_1\hat{\mathrm{P}}(\mathrm{S}) + c_2\hat{\mathrm{P}}(3)\,. \qquad (29)$$

This operator implies some degree of indistinguishability between system (S) and (3).

iii) Finally, if the third subsystem in the preceding model ii) is taken to be in a state approximately constant on the pertinent time-scale of (S) (for example, a highly excited coherent state of an oscillator or a strongly

pumped two-level system, see below), then, also this third system can be eliminated: As will be shown below, it will then enter the dynamics of the remaining $N = 1$- network approximately as a c-number only.

5 Trajectories

5.1 Quantum beats

5.1.1 Reduced system

Let us start by considering a three-level model, in which two decay channels, here $\hat{\mathrm{G}}_1(\mathrm{S}) = \hat{\mathrm{P}}_{12}(\mathrm{S})$, $\hat{\mathrm{G}}_2(\mathrm{S}) = \hat{\mathrm{P}}_{13}(\mathrm{S})$, exist. To allow for interference, leading to non-exponential decay (beat-frequency given by the energy-splitting of the decaying doublet) one has to introduce so-called non-secular terms into the evolution equations (Ref. [12]). Such non-secular terms imply non-diagonal elements in the parameter matrix, $D_{12} = D_{21}^*$ (D_{11} and D_{22} are real and positive). In the case of a Hydrogen-atom in an electrical field (eigenstates $|nlm\rangle$) the two upper levels could be the states $|2,1,0\rangle$ and $|2,0,0\rangle$ split by the linear Stark-effect, the third level the ground state $|1,0,0\rangle$.

One may wonder, what this non-exponentiality means for a single system: Do the decay rates become time-dependent?

To find the stochastic unraveling we first diagonalize the parameter matrix D_{ij}. The eigenvalues are

$$W_{1(2)} = \frac{1}{2}(D_{11} + D_{22}) \overset{+}{(-)} \sqrt{[\frac{1}{2}(D_{11} - D_{22})]^2 + |D_{12}|^2}\,, \tag{30}$$

which can be rewritten for identical damping rates $D_{11} = D_{22} = D$ as

$$W_{1(2)} = D \overset{+}{(-)} |D_{12}|. \tag{31}$$

With $D_{12} = r\,\mathrm{e}^{i\,\phi}$ the transformation matrix U is given by

$$U = \frac{1}{\sqrt{2}} \begin{pmatrix} \mathrm{e}^{i\phi} & -\mathrm{e}^{i\phi} \\ 1 & 1 \end{pmatrix}, \tag{32}$$

so that the transformed environment-operators are

$$\hat{\mathrm{F}}_1 = \frac{1}{\sqrt{2}}(\mathrm{e}^{i\phi}\hat{\mathrm{P}}_{12} + \hat{\mathrm{P}}_{13})\,, \tag{33}$$

$$\hat{\mathrm{F}}_2 = \frac{1}{\sqrt{2}}(-\mathrm{e}^{i\phi}\hat{\mathrm{P}}_{12} + \hat{\mathrm{P}}_{13})\,. \tag{34}$$

These new damping channels are still orthogonal but now independent from each other. Because of symmetry arguments [17], we require $D_{11} = D_{22} = D_{12} = r$, so that the transformed damping rates are: $W_1 = 2D, \quad W_2 = 0$. The resulting stochastic simulation is shown in Figure 2

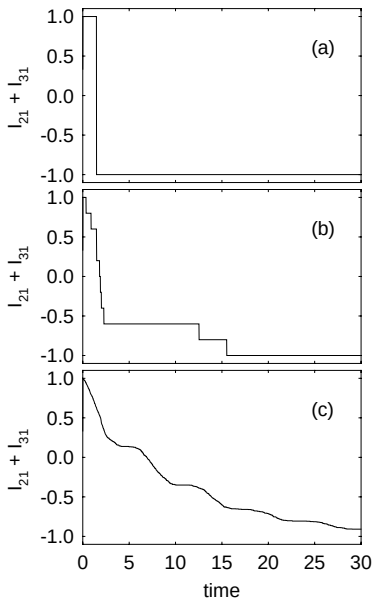

Fig. 2. Quantum beat trajectories of a three-level system. Shown is the inversion $I_{21} + I_{31}$ (for definition see Eq. (35)). Damping rate $W_1 = 2D = 0.2$, initial state $\frac{1}{\sqrt{2}}(|2\rangle + |3\rangle)$, (a) Single trajectory. (b) Average over 10 trajectories. (c) Average over 1000 trajectories. Here and in the following the model parameters are in reciprocal time units.

in terms of inversion parameters, where the inversion for a local transition (i, j) will be defined by

$$I_{ji}^{\mu} = \mathrm{Tr}\{\hat{\rho}\hat{\mathrm{I}}_{ji}(\mu)\}\,, \tag{35}$$

with $\hat{\mathrm{I}}_{ji}(\mu) = \hat{\mathrm{P}}_{jj}(\mu) - \hat{\mathrm{P}}_{ii}(\mu)$. Figure 2 shows the simulation of a single decay channel, which, despite a constant decay rate, is characterized by an oscillating decay probability depending on the momentary system state right before projection: If we take for simplicity $|\Psi\rangle = \sin\varphi|2\rangle + \cos\varphi|3\rangle$ we find according to equation (18) $P_1 = \frac{1}{2}(1 + \sin(2\varphi))\delta t$. These probability oscillations in time, though, become visible only after averaging over many simulations with identical initial state, which is reminiscent of the spatial interference pattern resulting for Young's double-slit experiment (*cf.* also [18] and references therein).

5.1.2 Full network

The scenario of the preceding section could be seen to result from a reduction of a $N = 2$ network as shown in Figure 1a with the coupling Hamiltonian

$$\begin{aligned}\hat{\mathrm{V}}(1,\mathrm{S}) = {} & \hbar C_{\mathrm{F}}^{1\mathrm{S}}\hat{\mathrm{P}}_{21}(1) \otimes (\hat{\mathrm{P}}_{12}(\mathrm{S}) + \hat{\mathrm{P}}_{13}(\mathrm{S})) \\ & + \hbar C_{\mathrm{F}}^{1\mathrm{S}*} P_{12}(1) \otimes (\hat{\mathrm{P}}_{21}(\mathrm{S}) + \hat{\mathrm{P}}_{31}(\mathrm{S}))\end{aligned} \tag{36}$$

and local damping W^1 in subsystem (1). There are two competing energy-transfer paths between the two subsystems such that a jump in (1) may have resulted from any of the two local transitions in (S), $|2\rangle \to |1\rangle$ and $|3\rangle \to |1\rangle$. For $W^1 \gg |C_{\rm F}|$ system (1) can adiabatically be eliminated, as described in Section 4.2, leading to $W^{\rm S}_{\rm eff} = 4|C_{\rm F}|^2/W^1$ to be identified with W_1.

5.2 Three-level cascades

5.2.1 Reduced system

Let us again focus on a three-level system, S, subject now to two damping channels constituting a cascade:

$$\begin{aligned} \hat{\rm L}_1 &= \sqrt{W_1}\,\hat{\rm F}_1 = \sqrt{W_1}\,\hat{\rm P}_{12}\,, \\ \hat{\rm L}_2 &= \sqrt{W_2}\,\hat{\rm F}_2 = \sqrt{W_2}\,\hat{\rm P}_{23}\,. \end{aligned} \tag{37}$$

W_1, W_2 are the corresponding transition rates. A corresponding simulation of quantum trajectories (under continuous coherent driving of the transition $|1\rangle \to |2\rangle$ with Ω_1 and the transition $|1\rangle \to |3\rangle$ with Ω_2) is shown in Figure 3a.

As an example for a transformation to non-orthogonal environment-operators we consider now the effect of the unitary transformation U defined by

$$U(\phi,\theta) = \begin{pmatrix} -\cos\phi\,{\rm e}^{i\theta} & \sin\phi \\ \sin\phi & \cos\phi\,{\rm e}^{-i\theta} \end{pmatrix}. \tag{38}$$

The transformed environment-operators will then be a superposition of the two original ones,

$$\hat{\tilde{\rm L}}_1 = -\cos\phi\,{\rm e}^{i\theta}\sqrt{W_1}\hat{\rm P}_{12} + \sin\phi\sqrt{W_2}\hat{\rm P}_{23}\,, \tag{39}$$

$$\hat{\tilde{\rm L}}_2 = \sin\phi\sqrt{W_1}\hat{\rm P}_{12} + \cos\phi\,{\rm e}^{-i\theta}\sqrt{W_2}\hat{\rm P}_{23}\,. \tag{40}$$

They are orthogonal for $W_1 = W_2$. Though the master equation is invariant under this transformation, the unraveling for $\hat{\rm L}_i$ and $\hat{\tilde{\rm L}}_i$, respectively, leads to qualitatively different quantum trajectories (Fig. 3b). While the simulation with $\hat{\rm L}_1$ and $\hat{\rm L}_2$ (Fig. 3a) shows the well known behaviour of the trajectory with projections into the lower levels of each damping channel, the trajectory based on the transformed environment-operators, $\hat{\tilde{\rm L}}_1$, $\hat{\tilde{\rm L}}_2$, is intuitively not clear: Both projected state and jump height differ from jump to jump. They depend on the state of the system right before projection. How could this behavior actually be implemented?

5.2.2 Full network

We consider a $N = 3$ network in which 3-level system (S) is supplemented by two damped two-level systems (damping constants W^1, W^3, see Fig. 1b), coupled *via*

$$\begin{aligned} \hat{\rm V}(1,{\rm S}) = {} & \hbar C_{\rm F}^{1{\rm S}}\hat{\rm P}_{21}(1)\otimes\hat{\rm P}_{23}({\rm S})\otimes\hat{\mathbf{1}}(3) \\ & + \hbar C_{\rm F}^{1{\rm S}^*}\hat{\rm P}_{12}(1)\otimes\hat{\rm P}_{32}({\rm S})\otimes\hat{\mathbf{1}}(3)\,, \end{aligned} \tag{41}$$

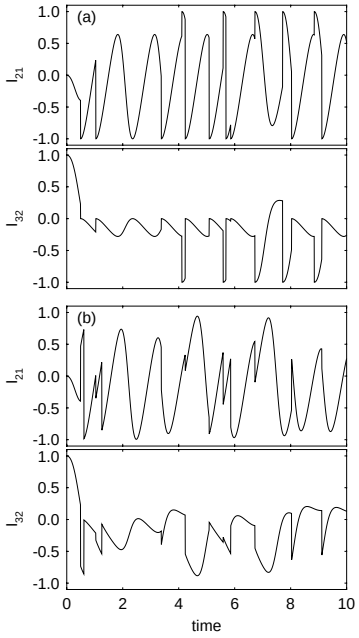

Fig. 3. Trajectories of the three-level cascade in terms of the inversion parameters I_{21}, I_{32} (see Eq. (35). Note that $I_{31} = I_{21} + I_{32}$.). Rabi-frequencies $\Omega_1 = 2$ and $\Omega_2 = 1.5$, respectively, damping rates $W_1 = W_2 = 3$. (a) Simulation with $\hat{\rm L}_1$ and $\hat{\rm L}_2$. (b) Simulation with transformed operators $\hat{\tilde{\rm L}}_1$ and $\hat{\tilde{\rm L}}_2$, for $\phi = \pi/2$ and $\theta = 0$.

$$\begin{aligned} \hat{\rm V}({\rm S},3) = {} & \hbar C_{\rm F}^{S3}\hat{\mathbf{1}}(1)\otimes\hat{\rm P}_{21}({\rm S})\otimes\hat{\rm P}_{12}(3) \\ & + \hbar C_{\rm F}^{{\rm S}3^*}\hat{\mathbf{1}}(1)\otimes\hat{\rm P}_{12}({\rm S})\otimes\hat{\rm P}_{21}(3)\,. \end{aligned} \tag{42}$$

In the large damping limit ($W^1 \gg |C_{\rm F}^{1{\rm S}}|, W^3 \gg |C_{\rm F}^{{\rm S}3}|$) the effective rates of the three-level system (S) are given by (*cf.* Eq. (25) and the Appendix A for $\delta = 0$)

$$W_1^{\rm S} = \frac{4C_{\rm F}^{1{\rm S}^*}C_{\rm F}^{1{\rm S}}}{W^1}\,, \tag{43}$$

$$W_2^{\rm S} = \frac{4C_{\rm F}^{{\rm S}3^*}C_{\rm F}^{{\rm S}3}}{W^3}\,, \tag{44}$$

which should be made to coincide with the original model parameters, W_1, W_2, respectively.

Now we will extend our consideration to the transformed environment-operators, equations (39, 40). In this case each auxiliary system is assumed to non-selectively couple to *each* transition of the three-level cascade (see Fig. 1c).

This means for the interaction Hamiltonians:

$$\begin{aligned}\hat{\tilde{\mathrm{V}}}(1,\mathrm{S}) &= \hbar\tilde{C}^{1\mathrm{S}}_{\mathrm{F}_2}\hat{\mathrm{P}}_{21}(1)\otimes\hat{\mathrm{P}}_{23}(\mathrm{S})\otimes\hat{\mathbf{1}}(3)\\ &+\hbar\tilde{C}^{1\mathrm{S}^*}_{\mathrm{F}_2}\hat{\mathrm{P}}_{12}(1)\otimes\hat{\mathrm{P}}_{32}(\mathrm{S})\otimes\hat{\mathbf{1}}(3)\\ &+\hbar\tilde{C}^{1\mathrm{S}}_{\mathrm{F}_1}\hat{\mathrm{P}}_{21}(1)\otimes\hat{\mathrm{P}}_{12}(\mathrm{S})\otimes\hat{\mathbf{1}}(3)\\ &+\hbar\tilde{C}^{1\mathrm{S}^*}_{\mathrm{F}_1}\hat{\mathrm{P}}_{12}(1)\otimes\hat{\mathrm{P}}_{21}(\mathrm{S})\otimes\hat{\mathbf{1}}(3)\,, \qquad (45)\\ \hat{\tilde{\mathrm{V}}}(\mathrm{S},3) &= \hbar\tilde{C}^{\mathrm{S}3}_{\mathrm{F}_2}\hat{\mathbf{1}}(1)\otimes\hat{\mathrm{P}}_{23}(\mathrm{S})\otimes\hat{\mathrm{P}}_{21}(3)\\ &+\hbar\tilde{C}^{\mathrm{S}3^*}_{\mathrm{F}_2}\hat{\mathbf{1}}(1)\otimes\hat{\mathrm{P}}_{32}(\mathrm{S})\otimes\hat{\mathrm{P}}_{12}(3)\\ &+\hbar\tilde{C}^{\mathrm{S}3}_{\mathrm{F}_1}\hat{\mathbf{1}}(1)\otimes\hat{\mathrm{P}}_{21}(\mathrm{S})\otimes\hat{\mathrm{P}}_{12}(3)\\ &+\hbar\tilde{C}^{\mathrm{S}3^*}_{\mathrm{F}_1}\hat{\mathbf{1}}(1)\otimes\hat{\mathrm{P}}_{12}(\mathrm{S})\otimes\hat{\mathrm{P}}_{21}(3)\,. \qquad (46)\end{aligned}$$

Our objective now is to choose the interaction parameters in such a way that this scenario can be interpreted as an implementation of the transformed damping operators. The structure of this transformation suggests restricting the parameters $\tilde{C}^{1\mathrm{S}}_{\mathrm{F}_1},...,\tilde{C}^{\mathrm{S}3}_{\mathrm{F}_2}$ in the following manner ($C_{\mathrm{F}_1}, C_{\mathrm{F}_2}$ real):

$$\tilde{C}^{1\mathrm{S}}_{\mathrm{F}_2} = \sin\phi\, C_{\mathrm{F}_2}\,, \qquad (47)$$

$$\tilde{C}^{1\mathrm{S}}_{\mathrm{F}_1} = -\cos\phi\, \mathrm{e}^{i\theta}C_{\mathrm{F}_1}\,, \qquad (48)$$

$$\tilde{C}^{\mathrm{S}3}_{\mathrm{F}_2} = \cos\phi\, \mathrm{e}^{-i\theta}C_{\mathrm{F}_2}\,, \qquad (49)$$

$$\tilde{C}^{\mathrm{S}3}_{\mathrm{F}_1} = \sin\phi\, C_{\mathrm{F}_1}\,. \qquad (50)$$

The parameters ϕ, θ of the original transformation can thus be expressed by the coupling constants of the extended model! It is shown in Appendix B that the coupling constants C_{F} can indeed be complex, and how the phase could be controlled.

The effective damping rates for the three-level system in the case of $W^1 = W^3 = W$ and $W \gg |C_{\mathrm{F}_i}|$ would be given by

$$W^{\mathrm{S}}_1 = \frac{4\tilde{C}^{1\mathrm{S}^*}_{\mathrm{F}_2}\tilde{C}^{1\mathrm{S}}_{\mathrm{F}_2}}{W} + \frac{4\tilde{C}^{\mathrm{S}3^*}_{\mathrm{F}_2}\tilde{C}^{\mathrm{S}3}_{\mathrm{F}_2}}{W} = \frac{4C^2_{\mathrm{F}_2}}{W}\,, \qquad (51)$$

$$W^{\mathrm{S}}_2 = \frac{4\tilde{C}^{1\mathrm{S}^*}_{\mathrm{F}_1}\tilde{C}^{1\mathrm{S}}_{\mathrm{F}_1}}{W} + \frac{4\tilde{C}^{\mathrm{S}3^*}_{\mathrm{F}_1}\tilde{C}^{\mathrm{S}3}_{\mathrm{F}_1}}{W} = \frac{4C^2_{\mathrm{F}_1}}{W}\,. \qquad (52)$$

The measurement as resulting from the two non-selective luminescence channels does not allow to assign a photon detection event to a specific transition. This undecidability leads to quite a different behaviour of the quantum trajectory than found for the original $\hat{\mathrm{L}}_1$, $\hat{\mathrm{L}}_2$.

5.3 c-number-shift

5.3.1 Reduced system

The unraveling of the master equation for the transformed operator, $\hat{\tilde{\mathrm{L}}} = \sqrt{W}(\hat{\mathrm{F}} + \alpha\hat{\mathbf{1}})$, leads to quantum trajectories of fundamentally different type, depending on α: P according to equation (18) reads here

$$P = P(\alpha=0) + [\alpha^*\left\langle\hat{\mathrm{F}}\right\rangle + \alpha\left\langle\hat{\mathrm{F}}^+\right\rangle + |\alpha|^2]W\delta t\,. \qquad (53)$$

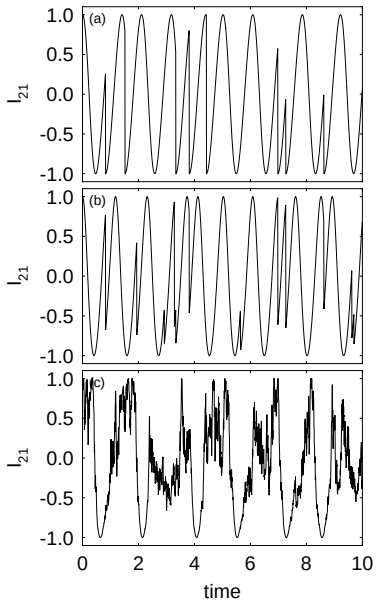

Fig. 4. Trajectories of a damped and resonantly driven two-level system in terms of the inversion I_{21} for different shift-values of α. Rabi-frequency $\Omega = 3$, damping rate $W = 3$. (a) $\alpha = 0$, (b) $\alpha = 0.5$, (c) $\alpha = 10$.

As shown in Figure 4, for a driven two-level system, the jump height of the individual projection becomes smaller with increasing modulus of α.

We now want to show that even this shift transformation can be seen to result from a reduced description of an extended network. We will see that also the effective Hamiltonian source term, equation (15), is indeed present.

For this purpose we consider an extended network consisting of a driven two-level system (S), coupled to a damping system (2), which, in turn, is coupled to a "dominating" third system (see Fig. 1d). Rather than considering a classical model for the third system (like is standard in homo/heterodyne spectroscopy based on a classical local oscillator [19]) we investigate two quantum models, a strongly driven two-level system, and a coherently prepared oscillator.

5.3.2 Full network

Describing the third system as a two-level system (see Fig. 1d) the interaction Hamiltonian consists of two coherent energy-transfer terms,

$$\begin{aligned}\hat{\mathrm{V}}(\mathrm{S},2) &= \hbar C^{\mathrm{S}2}_{\mathrm{F}}\hat{\mathrm{P}}_{21}(\mathrm{S})\otimes\hat{\mathrm{P}}_{12}(2)\otimes\hat{\mathbf{1}}(3)\\ &+\hbar C^{\mathrm{S}2^*}_{\mathrm{F}}\hat{\mathrm{P}}_{12}(\mathrm{S})\otimes\hat{\mathrm{P}}_{21}(2)\otimes\hat{\mathbf{1}}(3)\,, \qquad (54)\end{aligned}$$

$$\hat{\mathrm{V}}(2,3) = \hbar C_{\mathrm{F}}^{23}\hat{\mathbf{1}}(\mathrm{S}) \otimes \hat{\mathrm{P}}_{12}(2) \otimes \hat{\mathrm{P}}_{21}(3) + \hbar C_{\mathrm{F}}^{23^*}\hat{\mathbf{1}}(\mathrm{S}) \otimes \hat{\mathrm{P}}_{21}(2) \otimes \hat{\mathrm{P}}_{12}(3)\,. \quad (55)$$

System (3) is assumed to be driven very strongly, so that system (2) will get energy transferred mainly from (3); system (S) will contribute only very little. Qualitatively, this means that jumps in system (2) will be correlated with an updating in system (3) leading almost to its ground-state, whereas there will be very little effect on system (S): This is the reason why the evolution in system (S) is like a diffusion process.

One can easily relate the parameter α of the formal transformation to the parameters of this extended network. We note that the energy dissipated by system (2) comes from the systems (S) and (3). The average flux from system (3) can (in the limit of $W^2 \gg |C_{\mathrm{F}}^{23}|$) be approximated by

$$W_{\mathrm{eff}}^{3}\rho_{22}^{\bar{3}} = \frac{4|C_{\mathrm{F}}^{23}|^2}{W^2}\rho_{22}^{\bar{3}}\,, \quad (56)$$

which is independent of system (1). This contribution may be identified with the constant term appearing in equation (53), which is also independent of the actual state of system (S). This leads, identifying

$$W \to W_{\mathrm{eff}}^{\mathrm{S}} = \frac{4|C_{\mathrm{F}}^{\mathrm{S2}}|^2}{W^2} \quad (57)$$

to the following relation

$$W_{\mathrm{eff}}^{\mathrm{S}}|\alpha|^2 \cong \frac{4|C_{\mathrm{F}}^{23}|^2}{W^2}\rho_{22}^{\bar{3}}\,. \quad (58)$$

On the time scale of system (S) the dynamics of system (3) is very fast. So it is possible to average system (3) over time intervals which are still small for system (S). In the strong driving limit we can assume saturation (due to the high damping of system (2) the influence of entanglement on the occupation of system (3) will be negligible), *i.e.*

$$\rho_{22}^{\bar{3}} \to \frac{1}{2}\,. \quad (59)$$

Inserting equations (57) and (59) into equation (58), we get

$$|\alpha| \cong \frac{|C_{\mathrm{F}}^{23}|}{\sqrt{2}|C_{\mathrm{F}}^{\mathrm{S2}}|}\,. \quad (60)$$

In Figure 5 we demonstrate that the third system, indeed, acts also as an effective source term for system (S) (*cf.* Eq. (16)), which is not driven otherwise. In fact, this "cross-talk" is a non-local effect (in this full network) and derives from built-up of entanglement between the subsystems: Only then does the jump in system (2) update also system (S). The relevant part of the entanglement between subsystem (S) and (2) is conveniently described here in terms of the covariance (Ref. [12])

$$M^{\mathrm{S2}} = \mathrm{Tr}\{\hat{\rho}\hat{\mathrm{I}}_{21}(\mathrm{S})\hat{\mathrm{I}}_{21}(2)\} - I_{21}^{\mathrm{S}}I_{21}^{2}\,, \quad (61)$$

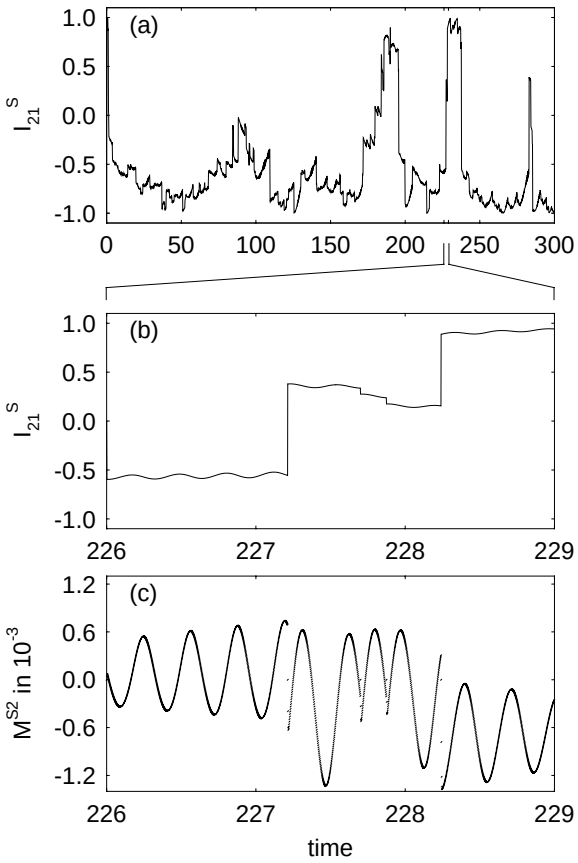

Fig. 5. Full network simulation according to Figure 1d. Rabi-frequencies $\Omega^{\mathrm{S}} = 0$ and $\Omega^{3} = 10$, damping rate $W^2 = 1000$, coupling coefficients $C_{\mathrm{F}}^{\mathrm{S2}} = 5$ and $C_{\mathrm{F}}^{23} = 20$. (a) Inversion I_{21}^{S} of system (S). (b) Inversion I_{21}^{S} of system (S) and the entanglement M^{S2} between system (S) and (2) on an enlarged time-scale.

where the inversion operator $\hat{\mathrm{I}}_{21}(\mu)$ has been defined in equation (35). We see that the direction of the jump depends on the sign of M^{S2} right before the jump. This indicates that a generalized but nominally local measurement model may, nevertheless, require entanglement in its actual full network implementation!

The output of the whole system is represented by the photons spontaneously emitted by subsystem (2). Here we consider the averaged photo-current rather than the single delta-like detection events produced by the simulation algorithm: we approximate this current between times t and $t + \Delta t$ by:

$$j(t + \Delta t) = j(t)\,\mathrm{e}^{-\beta\,\Delta t} + \beta J \quad (62)$$

with the smoothing parameter β. J is equal to 1, if there is a detection event during the interval Δt and 0 otherwise. This photo-current is found to be correlated with the quadrature component $\langle\hat{x}_\phi\rangle$ of the 2-level system with $\hat{x}_\phi = \frac{1}{2}(\hat{\mathrm{P}}_{12}\,\mathrm{e}^{-i\phi} + \hat{\mathrm{P}}_{21}\,\mathrm{e}^{i\phi})$ (*cf.* optical homodyne measurement [20]). Here, this phase ϕ is identified with the phase difference Θ of the coupling constants $C_{\mathrm{F}}^{\mu\nu}$, $C_{\mathrm{F}}^{\mathrm{S2}} \sim C_{\mathrm{F}}^{23}\mathrm{e}^{i\Theta}$ which is taken in our example to be $-\frac{\pi}{2}$. Figure 6 shows

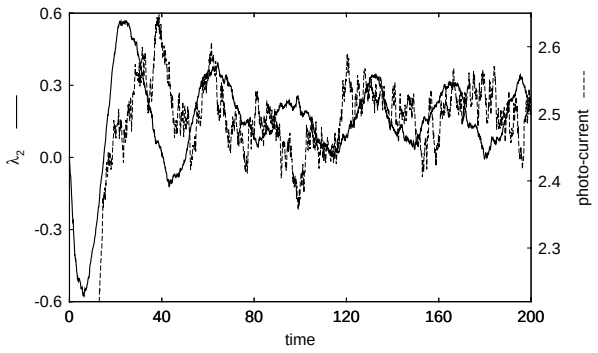

Fig. 6. Correlation between local coherence $\lambda_2^{\rm S} = i(\rho_{21}^{\rm S} - \rho_{12}^{\rm S})$ and the photo-current $j(t)$, as defined in equation (62). Parameters: $\Omega_{\rm S} = 0.1$, $\Omega_3 = 20$, $W_2 = 2000$, $C_{\rm F}^{\rm S2} = 4$, $C_{\rm F}^{23} = 50i$, $\beta = 0.2$, average over 100 single trajectories.

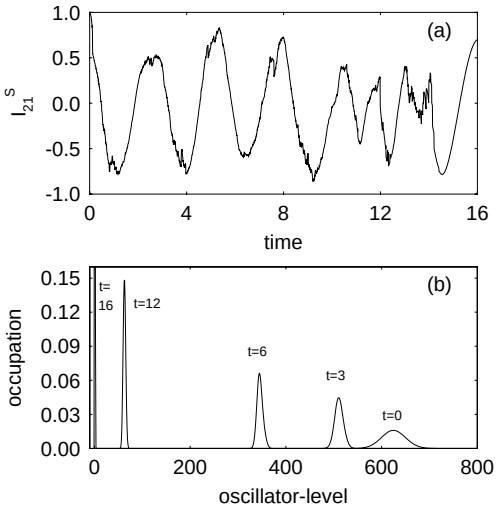

Fig. 7. Full network simulation according to Figure 1d, with system 3 replaced by an harmonic oscillator prepared in a coherent state with eigenvalue 25. (a) Inversion $I_{21}^{\rm S}$ of system S. (b) Occupation of the oscillator-levels at discrete instances of time. $\Omega^{\rm S} = 1$, $W^2 = 100$, $C_{\rm F}^{\rm S2} = 5$, $C_{\rm F}^{23} = 10$.

the correlation between $\langle \hat{x}_{-\pi/2} \rangle = i(\rho_{21}^{\rm S} - \rho_{12}^{\rm S})$, where $\rho_{ij}^{\rm S}$ is the reduced density matrix of subsystem S, and the photo-current. The correlation-index is 0.55. So, with the proposed scenario it is possible to perform a weak measurement of the instantaneous polarization of S, which would be inaccessible by direct detection schemes.

Alternatively, the third system may be modelled by a quantum mechanical harmonic oscillator, initially excited in a very high coherent state. In contrast to the strongly driven two-level system, no additional time scale comes in because there is no time-dependent driving field. On the other hand, this initial state will eventually decay.

The two interactions are, again, the resonant energy transfer couplings; $\hat{\rm V}({\rm S}, 2)$ is as given by equation (54), while $\hat{\rm V}(2, 3)$ reads in the present case

$$\begin{aligned}\hat{\rm V}(2,3) = {} & \hbar C_{\rm F}^{23} \hat{\mathbf{1}}({\rm S}) \otimes \hat{\rm P}_{12}(2) \otimes \hat{\rm a}^{+}(3) \\ & + \hbar C_{\rm F}^{23\,*} \hat{\mathbf{1}}({\rm S}) \otimes \hat{\rm P}_{21}(2) \otimes \hat{\rm a}(3)\,, \end{aligned} \tag{63}$$

with $\hat{\rm a}(3)$, $\hat{\rm a}^{+}(3)$ being the annihilation and the creation operators of the harmonic oscillator, respectively. (In the simulations given here, the harmonic oscillator is restricted to 1000 levels.) As shown in Figure 7, this harmonic oscillator-model also leads to a diffusive behavior of system (S), which is weakly driven in the present case. However, at the same time, the dissipation will cause the occupation of the harmonic oscillator state to decrease, so that the diffusive behaviour will end after some finite time, when the ground state has been reached (see Fig. 7). This behavior cannot be mapped onto the reduced description as defined by equation (53).

6 Photon counting

As has been shown in the previous chapters, different couplings to the environment lead to different kinds of trajectories, while, on the level of the ensemble description and the master equation, there may be no difference. However, the quantum trajectories enable the determination also of higher moments, which are not accessible through the master equation. As an example consider the Mandel Q-Parameter [21] for a luminescence channel i,

$$Q^i = \frac{\langle n_i^2 \rangle - \langle n_i \rangle^2}{\langle n_i \rangle} - 1, \tag{64}$$

and the degree of correlation between two luminescence channels with photon number n_i, $i = 1, 2$, defined by the covariance (*cf.* Ref. [22]),

$$R = \frac{\langle n_1 n_2 \rangle - \langle n_1 \rangle \langle n_2 \rangle}{\sqrt{{\rm var}(n_1)}\sqrt{{\rm var}(n_2)}} \tag{65}$$

where ${\rm var}(n_i) = \langle n_i^2 \rangle - (\langle n_i \rangle)^2$ and $\langle \dots \rangle$ denotes averaging over a sampling time $T \gg W^{-1}$. For uncorrelated photon channels we expect $R = 0$, for maximum correlated (anti-correlated) channels $R = 1$ ($R = -1$).

In the case of the three-level cascade (*cf.* Sect. 5.2) we demonstrate in Figure 8 the dependence of Q and R on the parameter ϕ (for $\theta = 0$), which controls the unitary transformation of the two damping channels, (Eqs. (39, 40)). We see that the photon-number fluctuations strongly reflect the type of trajectories. This example shows that interesting details of the quantum dynamical processes can be tested by means of local and coincidence – photon-counting studies. Experiments on this level could very sensitively discriminate between models, which, otherwise, might have a very similar ensemble behavior.

7 Summary and conclusions

We have been concerned with the interface between a quantum system and its measuring environment. Guided

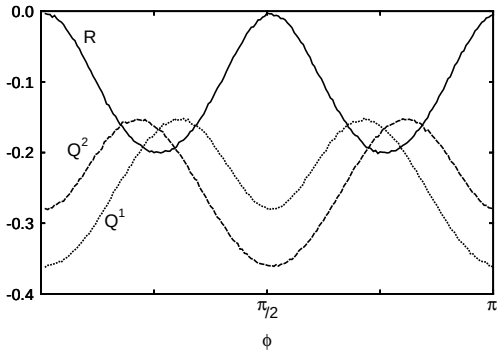

Fig. 8. Photon-counting statistics for the 3-level cascade as of Figure 3: Mandel Q-Parameters, Q^1, Q^2 for the two frequency channels, and normalized covariance R, as a function of ϕ. ϕ is the parameter in the unitary transformation as specified by equations (39), (40). Parameters are: $W_1 = W_2 = 3$, $\Omega_1 = 2$, $\Omega_2 = 1.5$, Sampling time: 1 time unit.

by the formal invariance properties of the Lindblad-master-equation we have explored a class of environment operators, which require extended networks for their implementation. In this sense, part of the environment still needs to be fully quantum. The examples of energy relaxation studied here include coherence effects, which are manifest in the quantum trajectories: Note that simple rate processes would confine all inversion parameters I_{ij} to ± 1. Different projection rules can be grouped into classes with the same ensemble behavior.

In all but one of the present examples the reduced model consisted just of one simple two- or three-level system. We considered two non-stationary (quantum beat, c-number-shift with an oscillator in a coherent initial state) and two stationary situations (cascade and c-number-shift with a driven 2-level system). Observations are to be distinguished according their ability to address first moments (the realm of the ensemble density matrix) or higher moments (controlled by details of the stochastic process). Only in the first example (quantum beats) does the coherence show up already in the measurement of the first moment (luminescence intensity).

Higher moments, which are not directly accessible to ensemble descriptions (noise properties, photon counting) are more sensitive to the details of the stochastic process. They are the only tools to distinguish processes which belong to the same class of ensemble behavior. This has been demonstrated for the cascade scenario, where the photon counting statistics depends on the transformed environment operators, which all produce the same ensemble result.

The c-number-shift examples, finally, show that not only discontinuous jumps, but also a diffusive motion can be implemented in open, discrete systems. In this case the measurement signal is correlated with the instantaneous polarization of the quantum object (S).

This network approach can be extended to situations in which the reduced system would not be a simple system but still constitute an effective network with $N \geq 2$. The c-number-shift model with an initially coherent oscillator state is of that type: In this case the decaying oscillator presents a fixed boundary condition for the subsystem (S) only at the beginning, while its own dynamics cannot be neglected at later times.

We thank J. Schlienz and R. Wawer for valuable discussions. Financial support by the Deutsche Forschungsgemeinschaft is gratefully acknowledged.

Appendix A: Effective damping rate of two coupled two-level systems

We consider a network of two two–level systems coupled via the coherent energy transfer interaction. System (S) is driven coherently. The respective Hamiltonian reads

$$\hat{\mathrm{H}} = \hat{\mathrm{H}}_0^{(\mathrm{S})} + \hat{\mathrm{H}}_0^{(2)} + \hat{\mathrm{H}}_{C_\mathrm{F}}^{(\mathrm{S},2)} + \hat{\mathrm{H}}_\Omega^{(\mathrm{S})}$$

with ($\hbar = 1$)

$$\hat{\mathrm{H}}_0^{(\mathrm{S})} = \frac{\omega^{(\mathrm{S})}}{2}(\hat{\mathrm{P}}_{22}(\mathrm{S}) - \hat{\mathrm{P}}_{11}(\mathrm{S})) \tag{66}$$

$$\hat{\mathrm{H}}_0^{(2)} = \frac{\omega^{(2)}}{2}(\hat{\mathrm{P}}_{22}(2) - \hat{\mathrm{P}}_{11}(2)) \tag{67}$$

$$\hat{\mathrm{H}}_{C_\mathrm{F}}^{(\mathrm{S},2)} = C_\mathrm{F}\hat{\mathrm{P}}_{21}(\mathrm{S})\hat{\mathrm{P}}_{12}(2) + {C_\mathrm{F}}^*\hat{\mathrm{P}}_{12}(\mathrm{S})\hat{\mathrm{P}}_{21}(2) \tag{68}$$

$$\hat{\mathrm{H}}_\Omega^{(\mathrm{S})} = \Omega[\hat{\mathrm{P}}_{21}(\mathrm{S})\mathrm{e}^{-i\omega t} + \hat{\mathrm{P}}_{12}(\mathrm{S})\mathrm{e}^{i\omega t}]\,. \tag{69}$$

Including damping in subsystem (2) (damping constant γ) the master equation is given by

$$\frac{\partial}{\partial t}\hat{\rho} = -\,i[\hat{\mathrm{H}},\hat{\rho}] + \frac{\gamma}{2}[2\hat{\mathrm{P}}_{12}(2)\hat{\rho}\hat{\mathrm{P}}_{21}(2) \tag{70}$$

$$-\,\hat{\mathrm{P}}_{21}(2)\hat{\mathrm{P}}_{12}(2)\hat{\rho} - \hat{\rho}\hat{\mathrm{P}}_{21}(2)\hat{\mathrm{P}}_{12}(2)]. \tag{71}$$

All operators can be expressed in the product basis $|1,1\rangle$, $|1,2\rangle$, $|2,1\rangle$ and $|2,2\rangle$, where the first index refers to system (S), the second to system (2).

The Hamilton operator after transformation into a rotating reference frame then is

$$\hat{\mathrm{H}} = \begin{pmatrix} \frac{-\delta^{(\mathrm{S})}-\delta^{(2)}}{2} & 0 & \Omega & 0 \\ 0 & \frac{-\delta^{(\mathrm{S})}+\delta^{(2)}}{2} & C_\mathrm{F}^* & \Omega \\ \Omega & C_\mathrm{F} & \frac{\delta^{(\mathrm{S})}-\delta^{(2)}}{2} & 0 \\ 0 & \Omega & 0 & \frac{\delta^{(\mathrm{S})}+\delta^{(2)}}{2} \end{pmatrix} \tag{72}$$

with $\delta^{(\mathrm{S})} = \omega^{(\mathrm{S})} - \omega$ and $\delta^{(2)} = \omega^{(2)} - \omega$.
The density matrix can be expressed as

$$\hat{\rho} = \sum_{i,j,m,n=1}^{2} \rho_{ij,mn}\hat{\mathrm{P}}_{im}^{(\mathrm{S})} \otimes \hat{\mathrm{P}}_{jn}^{(2)}. \tag{73}$$

We are interested in system (S) and calculate its reduced density matrix, ($\mathrm{Tr}_2\{\dots\}$ means trace over system (2))

$$\hat{\rho}_2 = \mathrm{Tr}_2(\hat{\rho}) = \begin{pmatrix} \rho_{11,11} + \rho_{12,12} & \rho_{11,21} + \rho_{12,22} \\ \rho_{21,11} + \rho_{22,12} & \rho_{21,21} + \rho_{22,22} \end{pmatrix}. \tag{74}$$

Assuming strong damping in subsystem (2) ($\gamma \gg C_{\rm F}$), we can restrict ourselves to

$$\hat{\rho}_2 \sim \begin{pmatrix} \rho_{11,11} & \rho_{11,21} \\ \rho_{21,11} & \rho_{21,21} \end{pmatrix}. \tag{75}$$

The evolution equations for these components are

$$\begin{aligned}
\dot{\rho}_{11,11} &= -i\Omega(\rho_{21,11} - \rho_{11,21}) + \gamma\rho_{12,12} \\
\dot{\rho}_{21,21} &= -i\Omega(\rho_{11,21} - \rho_{21,11} + \rho_{22,21} - \rho_{21,22}) \\
&\quad -i({C_{\rm F}}^*\rho_{12,21} - C_{\rm F}\rho_{21,12}) + \gamma\rho_{22,22} \\
\dot{\rho}_{21,11} &= -i\Omega(\rho_{11,11} - \rho_{21,21} + \rho_{22,11}) - i{C_{\rm F}}^*\rho_{12,11} \\
&\quad -i\delta^{(\rm S)}\rho_{21,11} + \gamma\rho_{22,12}.
\end{aligned} \tag{76}$$

To get closed equations, we also need the evolution of the following variables:

$$\begin{aligned}
\dot{\rho}_{12,11} &= -i\delta^{(2)}\rho_{12.11} - iC_{\rm F}\rho_{21,11} + i\Omega\rho_{12,21} - \frac{1}{2}\gamma\rho_{12,11} \\
\dot{\rho}_{12,21} &= i\delta^{(\rm S)}\rho_{12,21} - i\delta^{(2)}\rho_{12,21} - iC_{\rm F}\rho_{21,21} + iC_{\rm F}\rho_{12,12} \\
&\quad +i\Omega(\rho_{12,11} + \rho_{12,22}) - \frac{1}{2}\gamma\rho_{12,21} \\
\dot{\rho}_{12,12} &= -iC_{\rm F}\rho_{21,12} + i{C_{\rm F}}^*\rho_{12,21} - \gamma\rho_{12,12}.
\end{aligned} \tag{77}$$

These equations are solved making use of the Laplace-transformation:

$$L[f(t)] = \tilde{f}(s) = \int_0^\infty {\rm e}^{-st} f(t)\,{\rm d}t$$

with its inverse

$$f(t) = \frac{1}{2\pi i}\int_{\Gamma-i\infty}^{\Gamma+i\infty} {\rm e}^{st}\tilde{f}(s)\,{\rm d}s.$$

With the transformation of the time derivative of $f(t)$,

$$L[\dot{f}(t)] = s\,\tilde{f}(s) - f(0)$$

the Laplace-transformed evolution equations read:

$$\begin{aligned}
&\tilde{\rho}_{12,11}(s + i\delta^{(2)} + \frac{\gamma}{2}) - \rho_{12,11}(t=0) \\
&\quad = -iC_{\rm F}\tilde{\rho}_{21,11} + i\Omega\tilde{\rho}_{12,21}
\end{aligned} \tag{78}$$

$$\begin{aligned}
&\tilde{\rho}_{12,21}(s - i\delta^{(\rm S)} + i\delta^{(2)} + \frac{\gamma}{2}) - \rho_{12,21}(t=0) \\
&\quad = -iC_{\rm F}\tilde{\rho}_{21,21} + i\Omega(\tilde{\rho}_{12,11} + \tilde{\rho}_{12,22}) + iC_{\rm F}\tilde{\rho}_{12,12}
\end{aligned} \tag{79}$$

$$\begin{aligned}
&\tilde{\rho}_{12,12}(s + \gamma) - \rho_{12,12}(t=0) \\
&\quad = -iC_{\rm F}\tilde{\rho}_{21,12} + iC_{\rm F}{}^*\tilde{\rho}_{12,21}.
\end{aligned} \tag{80}$$

With the the damped system being initially in the ground state, we have $\rho_{21,21}(t=0) = 1$.

Substituting equation (78) into equation (79) and neglecting terms of the order $\Omega C_{\rm F}$ and Ω^2 ($\Omega \ll \gamma$) we get

$$\begin{aligned}
\tilde{\rho}_{12,12} = -\frac{2{C_{\rm F}}^*C_{\rm F}}{s+\gamma}\frac{s+\gamma/2}{(s+\gamma/2)^2 + (\delta^{(2)} - \delta^{(\rm S)})^2} \\
\times(\tilde{\rho}_{12,12} - \tilde{\rho}_{21,21})
\end{aligned} \tag{81}$$

so that

$$\rho_{12,12}(t) = \frac{|C_{\rm F}|^2}{(\gamma/2)^2 + (\delta^{(\rm S)} - \delta^{(2)})^2}\rho_{21,21}(t) \tag{82}$$

and the first equation of (76) reduces to

$$\begin{aligned}
\dot{\rho}_{11,11} = -i\Omega(\rho_{21,11} - \rho_{11,21}) + \gamma\frac{|C_{\rm F}|^2}{(\gamma/2)^2 + (\delta^{(\rm S)} - \delta^{(2)})^2} \\
\times\rho_{21,21}(t).
\end{aligned} \tag{83}$$

The effective damping rate for the system (S),

$$W_{\rm eff} = \frac{|C_{\rm F}|^2\gamma}{(\gamma/2)^2 + (\omega^{\rm S} - \omega^2)^2} \tag{84}$$

represents a Lorentzian of width γ with respect to the detuning between (S) and (2). Remember that this result is valid only for $\Omega\ ,\ C_{\rm F} \ll \gamma$.

Appendix B: Complex coupling constant

Can the conditions (47) - (50) be realized, in principle? As shown in [23] the coupling $C_{\rm F}$ between two subsystems (local energy levels (i,l) and (j,k), respectively) derives from the non-local Coulomb-interaction: up to dipole-dipole contributions we find

$$C_{\rm F}(ijkl) = \frac{{\rm e}^2}{4\pi\epsilon\epsilon_0 R^3}\left[\mathbf{P}_{il}\mathbf{P}_{jk} - \frac{3}{R^2}(\mathbf{R}\cdot\mathbf{P}_{il})(\mathbf{R}\cdot\mathbf{P}_{jk})\right] \tag{85}$$

where $\mathbf{R} = R\mathbf{e}_z$ is the vector connecting the two subsystems, and the dipole (transition) matrix elements are given by the vectors

$$\mathbf{P}_{il} = \int {\rm d}^3x\ \Phi_i^*(\mathbf{x})\mathbf{x}\Phi_l(\mathbf{x}). \tag{86}$$

The transfer of electronic excitation from one subsystem to the other, as considered in the last section, corresponds to $i \neq l\ ,\ j \neq k$ and $l, j > i, k$. This process is efficient only if the excitation energies of the two subsystems are close to each other (resonance). For nondegenerate subsystems see the Appendix A.

As can be seen from equation (85), arbitrary complex phases can be realized by appropriate relative orientation of the two dipole-vectors representing the interacting subsystems.

To see this, consider Hydrogen-like wavefunctions and take the transition from $\Phi_1 = \Psi_{1,0,0}$ (*i.e.* $n=1,\ l=0,\ m=0$) to $\Phi_2 = \Psi_{2,1,1}$ in one subsystem and the transition from $\Phi_4 = \Psi_{2,1,1}$ to $\Phi_3 = \Psi_{1,0,0}$ in the other subsystem. The two pertinent dipole-matrix elements then are

$$\mathbf{P}_{12} = \frac{d}{\sqrt{6}}(-1,\ i,\ 0) \tag{87}$$

$$\mathbf{P}_{43} = \frac{d}{\sqrt{6}}(-1,\ -i,\ 0) \tag{88}$$

with $d = \frac{256}{81}\frac{1}{\sqrt{6}}\frac{\hbar^2}{me^2}4\pi\epsilon_0$.
Rotation of the vector $\mathbf{P}_{43}$ in the xy-plane by the angle Θ gives

$$\mathbf{P}_{43} = \frac{d}{\sqrt{6}}\begin{pmatrix} -\cos\Theta + i\sin\Theta \\ -i\cos\Theta - \sin\Theta \\ 0 \end{pmatrix} = \frac{d}{\sqrt{6}}\,\mathrm{e}^{-i\Theta}\begin{pmatrix} -1 \\ -i \\ 0 \end{pmatrix} . \tag{89}$$

Inserting equations (89) and (87) into equation (85) we obtain

$$C_{\mathrm{F}}(1212) = \frac{\mathrm{e}^2}{4\pi\epsilon\epsilon_0 R^3}\frac{d^2}{3}\mathrm{e}^{-i\Theta} . \tag{90}$$

References

1. K. Blum, *Density Matrix Theory and Applications* (Plenum Press, New York 1981).
2. M. Rigo, N. Gisin, Quant. Semicl. Optics **8** (1996).
3. Special Issue on Stochastic Quantum Optics, Quantum and Semicl. Optics **8**, 47 (1996).
4. J. Pöttinger, K. Lendi, Phys. Rev. A **3**1, 1299 (1985).
5. V. Gorini, A. Kossakowski, E.C.G. Sudarshan, J. Math. Phys. **1**7, 821 (1976).
6. G. Lindblad, Math. Phys. **4**8, 119 (1976).
7. R. Alicki, K. Lendi, *Lecture notes in physics 286* (Springer, Berlin, Heidelberg, New York, 1987).
8. J.K. Breslin, G.J. Milburn, H.M. Wiseman, Phys. Rev. Lett. **7**4, 4827 (1995).
9. J. Dalibard, Y. Castin, K. Mølmer, Phys. Rev. Lett. **6**8, 580 (1992).
10. K. Mølmer, Y. Castin, J. Dalibard, J. Opt. Soc. Am. B **1**0, 524 (1993).
11. H. Carmichael, *An Open Systems Approach to Quantum Optics* (Springer, Berlin, Heidelberg, New York, 1993).
12. G. Mahler, V.A. Weberruß, *Quantum Networks: Dynamics of Open Nanostructures* (Springer, Berlin, Heidelberg, New York, 1995).
13. R. Dum, A.S. Parkins, P. Zoller, C.W. Gardiner, Phys. Rev. A **4**6, 4382 (1992).
14. G. Mahler, M. Keller, R. Wawer, Eur. Phys. J. D **1**, 15 (1998).
15. M. Keller, G. Mahler, J. mod. Optics **4**1, 2537 (1994).
16. T. Förster, Annalen der Physik (Leipzig)(b) **2**, 55 (1948).
17. A. Bohle, Diploma Thesis, Universität Stuttgart (1993).
18. G.C. Hegerfeldt, M.B. Plenio, Quantum Optics **6**, 15 (1994).
19. U. Leonhardt, M. Munroe, T. Kiss, Th. Richter, M.G. Raymer, Opt. Commun. **1**27, 144 (1996).
20. D.T. Smithey *et al.*, Phys. Rev. Lett. **7**0, 1244 (1993).
21. see, *e.g.*, D.F. Walls, G.J. Milburn, *Quantum Optics* (Springer, Berlin, Heidelberg, New York, 1994).
22. G. Mahler, R. Wawer, Superlattices and Microstructures **2**1, 7 (1997).
23. W.G. Teich, K. Obermayer, G. Mahler, Phys. Rev. B **3**7, 8111 (1988).